

Bridged Lamellae: Crystal Structure(s) of Low Molecular Weight Linear Polyethylene

Douglas L. Dorset

Electron Diffraction Department, Hauptman-Woodward Institute, 73 High Street, Buffalo, New York 14203-1196

Received August 31, 1998; Revised Manuscript Received November 7, 1998

ABSTRACT: The crystal structure of a low molecular weight polyethylene ($M_w = 595$) with low polydispersity (1.11) was determined from electron diffraction intensity data collected from samples epitaxially oriented on benzoic acid and subsequently annealed. A distribution of local microcrystalline structures was observed, somewhat resembling orthorhombic *n*-paraffins: $n\text{-C}_{37}\text{H}_{76}$ to $n\text{-C}_{44}\text{H}_{90}$. However, a quantitative structure determination based on the $0kl$ single-crystal intensities reveals that the lamellae are not totally separated in the microcrystalline array, apparently due to residual bridging molecules that span adjacent chain layers. An atomic model for a frequently observed structure, comparable to $n\text{-C}_{41}\text{H}_{84}$, packs in space group $A2_1am$ with $a = 7.42$, $b = 4.96$, and $c = 109.80$ Å and corresponds well to the observed diffraction amplitudes ($R = 0.21$).

Introduction

Recently, electron crystallographic techniques have been employed to determine the crystal structures of *n*-paraffin solid solutions.^{1,2} Samples oriented epitaxially on substrates such as benzoic acid or naphthalene will produce single-crystal electron diffraction patterns^{3,4} to reveal local variations of lamellar structure (lamellar thickness and symmetry). From a concentration series of two paraffin components, it has been shown⁵ that the average unit cell symmetries of stable solid solutions do not necessarily obey the rules stipulated by Kitai-gorodskii,⁶ i.e., that the average space group should be either lower or the same as those found for the pure components. In fact, there is no such thing as continuity of symmetry for a concentration series of the same two components that form stable binary solid solutions, since local microcrystalline domains can have their own distinct crystal structures. In general, any intermediate solid solution will have an orthorhombic structure in space group $Pca2_1$, if it mimics an even-chain paraffin, or space group $A2_1am$, if it mimics an odd-chain paraffin. The lamellar spacings for the solid solutions also lie very close to the values identified for the corresponding pure orthorhombic paraffin polymorph.⁵

In two X-ray analyses of binary paraffin solid solutions,^{7,8} it was proposed that the mixed chain lamellar surfaces could contain methyl group protrusions, leading to a nonplanar limiting surface for each lamella. This claim was tested in a three-dimensional electron diffraction analysis of similar solid solutions,² yielding results that were supported by surface decoration experiments and atomic force microscopy.⁹ These results favored the opposite conclusion that the lamellar surface would terminate as a plane that, on average, would be nearly flat on an atomic scale. This model would require conformational disorder at the ends of the longer chains, a feature indicated by vibrational spectroscopic measurements.¹⁰

Very little structural difference was experienced when paraffin wax fractions from petroleum were analyzed in the same way.^{11,12} Again, the single-crystal electron diffraction patterns from epitaxially oriented samples resembled those from pure paraffins, except that the

limited resolution of the low-angle reflections (found also for the patterns from binary solid solutions) indicated a distribution of chain lengths in a single lamella. The perfection and high resolution of the diffraction patterns from local microareas indicated that the stacking of adjacent lamellae should be highly correlated, even though the corresponding (001) crystallographic plane is the least ordered in the whole structure. Recently, the three-dimensional crystal structure of a paraffin wax¹³ supported conclusions drawn from earlier two-dimensional analyses, i.e., that polydispersity, in itself, did not affect the crystallization of paraffin solid solutions.

It is reasonable to expect that the crystallization of low molecular weight linear polyethylene should closely mimic the petroleum waxes, particularly if the constituent lamellae contain extended chains. If the polydispersity of the chain-length distribution is suitably low, a well-resolved lamellar packing might be expected again so that the designation “wax” or “polyethylene” would only denote the synthetic or natural origin of a paraffin chain mixture but otherwise be an artificial distinction between very similar materials. As will be shown in a quantitative crystal structure analysis of a low molecular weight polyethylene, the distinction between waxes and the low molecular weight polymer may, in fact, be more important than mere nomenclature.

Materials and Methods

Polyethylene Crystallization. A low molecular weight linear polyethylene standard, PE600, obtained from Scientific Polymer Products, Inc. (Ontario, NY), was stated to have the values: $M_w = 595$, $M_n = 535$, and $M_p = 565$, corresponding to a polydispersity of 1.11. Its DSC melting behavior, measured on a Mettler TA 3300 instrument, was nearly enantiotropic (Figure 1), with a broad endotherm peaking at 75.8 °C. Consistent with the number average chain length, binary solids of the linear polyethylene with $n\text{-C}_{37}\text{H}_{76}$ were shown to form solid solutions by the linear continuity of the melting temperature with concentration (Dorset, D. L., unpublished results).

Dilute solutions of the polyethylene made up in various solvents (*p*-xylene, light petroleum) were used to prepare

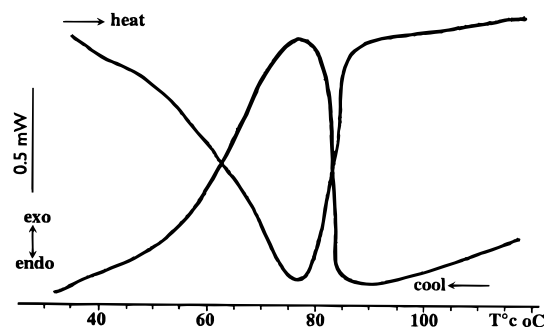
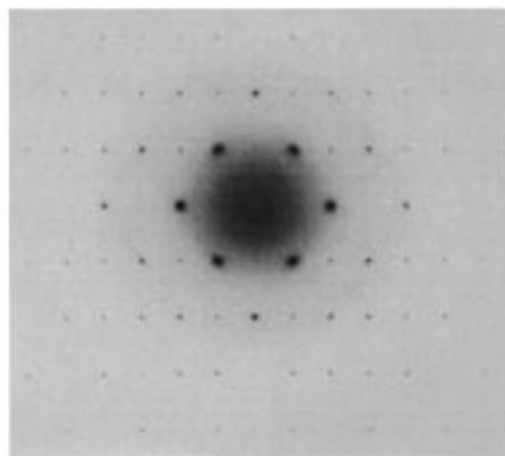
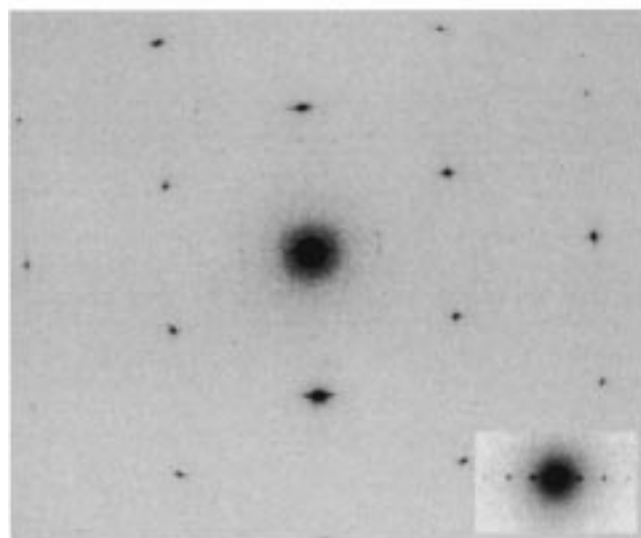


Figure 1. DSC heating/cooling scans (5 °C/min) for PE600 (1.54 mg sample).



(a)



(b)

Figure 2. Electron diffraction patterns from PE600: (a) $hk0$ pattern from lamellae crystallized from dilute solution. (a^* is horizontal; b^* is vertical); (b) $0kl$ pattern from samples epitaxially crystallized on benzoic acid (c^* is horizontal; b^* is vertical) and annealed at 60 °C for 6 h. (Inset shows detail of low-angle $00l$ row.)

microcrystals for electron diffraction experiments. When evaporated onto a carbon-film-covered electron microscope grid, thin-layer crystals were formed with a well-developed (001) face, giving a characteristic $hk0$ pattern (Figure 2a). These lamellae had also been decorated with polyethylene vapors in an earlier study.⁹

When evaporated onto a mica sheet, the polyethylene film could be covered with benzoic acid crystals for epitaxial orientation, using a modification of the procedure described

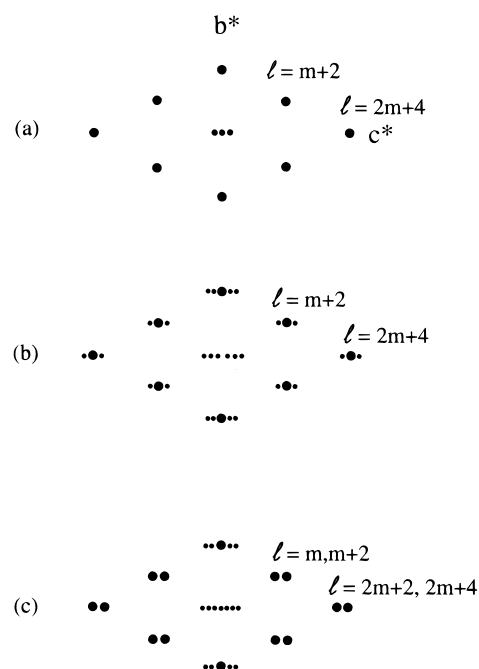


Figure 3. Schematic view of $0kl$ electron diffraction patterns from epitaxially oriented polydisperse n -paraffin solid solution (see also ref 21): (a) mostly "nematic" order of chains with only beginnings of lamellar order; (b) ordered lamellar chain packing but molecular bridges across lamellae force the interlamellar gap to be $3(c_s/2)$; (c) ordered lamellar packing but with gap distance not an integral multiple of $c_s/2$.

by Wittmann, Hodge, and Lotz.⁴ The binary organic mixture was melted between two mica sheets on a thermal gradient to allow the liquid to flow initially over carbon-film-covered electron microscope grids before cooling to recrystallize the eutectic solid. When cooled, the sandwich could be split to expose the organic solid, so that the benzoic acid could be removed subsequently by sublimation in vacuo. Alternatively, the organic material could be annealed on a Mettler FP82 microscope hot stage, controlled by an FP90 central processor. After cooling the sandwich was opened as before for removal of the benzoic acid. The annealing temperature selected was 60 °C for 6 h.

Electron Diffraction. Selected area electron diffraction experiments were carried out at 100 kV with a JEOL JEM-100CX II electron microscope, following usual low-dose procedures for the examination of organic materials.¹⁴ Patterns were recorded on CEA Reflex 25 screenless X-ray film, developed with Industrex developer.

Relative positions of diffraction spots on the patterns were measured with a Charles Supper (Natick, MA) circular film reading device. As described before, and illustrated in Figure 3, the spacings of the low-angle $00l$ reflections were used to determine the average lamellar thicknesses for local microcrystalline areas. These could be compared to the values expected for the pure orthorhombic n -paraffins.¹⁵ Ultimately the diffraction spacings were calibrated against the (111) spacing of a gold powder pattern used as an internal standard. However, since the (020) spacing of n -paraffins in the orthorhombic layer does not vary greatly (e.g., typically <1%) in binary paraffin solids,¹⁶ the $d_{020} = 2.48$ Å was used as a secondary standard for these measurements without significant error.

Intensities were measured by scans of the patterns on a Joyce-Loebl Mk.IIIC flat-bed microdensitometer. A triangular approximation to the peak area was made on the resulting plots to estimate the relative intensities. No Lorentz correction was applied.¹⁴ Intensities in patterns from similar structures were averaged over symmetry-related reflections and over separate patterns to obtain an estimate of true integrated values.¹⁷

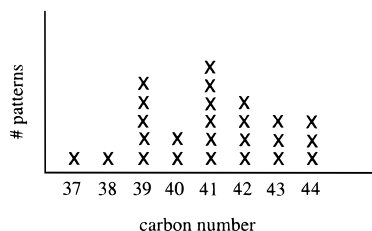


Figure 4. Distribution of representative lamellar carbon numbers in microareas of oriented PE600. For multiple samples, the lamellar thicknesses are determined from the diffraction patterns to be as follows: C39, 52.37 ± 0.43 (51.52 Å); C40, 53.77 ± 0.12 (52.65 Å); C41, 54.90 ± 0.37 (54.07 Å); C42, 55.92 ± 0.28 (55.19 Å); C43, 57.47 ± 0.45 (56.61 Å); C44, 58.34 ± 0.27 (57.73 Å). Parenthetical values are those predicted by Nyburg and Potworowski¹⁵ for the corresponding pure orthorhombic *n*-paraffin.

Crystal Structure Analysis. A qualitative appraisal of the average layer structure could be obtained from the relative indices of intense 01/ and 00/ reflections related to the strong $0k/$ peaks from polyethylene (Figure 3). In principle, these indices are directly related to the analogous carbon number m (i.e., $n\text{-C}_m\text{H}_{2m+2}$, abbreviated *C_m*) of the average lamella.⁵ Its theoretical spacing,¹⁵ e.g., $1.27m + 1.85$ Å, should be very close to the measured value. Also, the extinction rules for indices of these reflections will indicate the space group of the unit cell.¹⁸

Atomic positions in the unit cell were initially determined by computing a one-dimensional Fourier transform with the 00/ reflections. A crystallographic phase envelope for an analogous pure paraffin structure (which can be determined by direct methods¹⁹) was used to provide approximately centrosymmetric values (0, π) to these reflections, however, testing the phase for the strongest 00/ "polyethylene" reflection. This analysis provided z/c positions for the carbons in the lamella, and (x/a or) y/b positions were inferred from the values of analogous orthorhombic *n*-paraffins. The heights of the peaks from the one-dimensional transform assisted in the determination of an average occupancy model for the outer chain positions.

Results

Before annealing, diffraction patterns from epitaxially crystallized samples initially revealed that the polymer could be oriented on benzoic acid in lamellar arrays. However, only 1 or 2 orders of the low-angle lamellar repeat were observed in these patterns, and these were often streaked along c^* . Annealing produced much more highly ordered samples (Figure 2b) in which 3 or 4 orders of the lamellar spacing were commonly observed in the rectangular $0k/$ diffraction patterns. In addition, the remaining "polyethylene" reflections were observed as sharp spots instead of arcs and to high resolution. Consistent with the molecular weight range given by the manufacturer, the distribution of lamellar spacings, and hence comparable parent crystal structure (Figure 4), was expressed by carbon numbers from C37 to C44, and the measured spacings were very close to values predicted by Nyburg and Potworowski¹⁵ for the orthorhombic paraffins.

Closer examination of the $0k/$ patterns, on the other hand, revealed a feature not observed previously for simple binary paraffin solid solutions^{1,5} or for the refined petroleum waxes.^{11,12} As is depicted in Figure 3b, there was only single strong "polyethylene" reflections observed, instead of doublets, and these were generally flanked by two weaker satellite peaks on the 00/ or 01/ rows. The indices of the strong peaks followed the rules $m + 2$ for the 01/ row and $2m + 4$ for the 00/ row for a

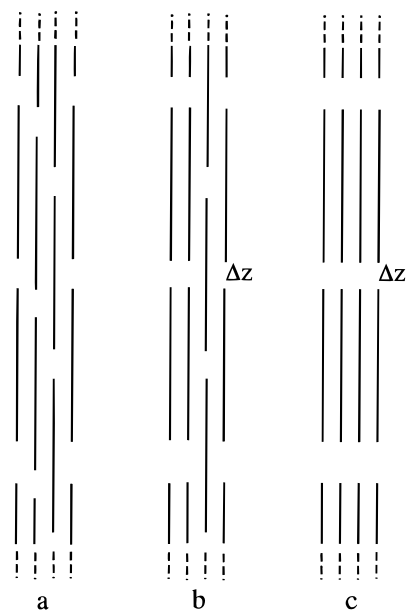


Figure 5. Schema of possible chain packing arrays for linear chains in solid solutions (where paraffinic chains are represented as straight lines): (a) "Nematic"-type order, where there are no average lamellae. (b) Nascent lamellae but also a fraction of bridging molecules spanning them. The value of Δz is constrained by the polymethylene repeat. (c) Stable lamellae, no bridging chains. The Δz value is no longer related to the polymethylene repeat and is determined only by the van der Waals interactions across the lamellar interfaces.

carbon number $n\text{-C}_m\text{H}_{2m+2}$, indicated by the corresponding lamellar spacing. Nevertheless, the extinction rules for the reflections¹⁸ were consistent still with space group $Pca2_1$ or $A2_1am$ if the carbon numbers were respectively even or odd. This behavior had been observed before during the annealing of polymethylene chains that had been deposited from the vapor phase onto an epitaxial substrate.²⁰ As shown schematically in Figure 5a, the initial "nematic"-like chain packing produced a diffraction pattern similar to Figure 3a, except that no lamellar reflections were observed; i.e., the pattern strongly resembles those from chain-folded polyethylene.²¹ With annealing in the presence of the nucleating substrate, a nascent lamellar packing was found (Figure 5b), producing patterns first resembling Figure 3a and then more like Figure 3b. The strong $0k/$ "polyethylene" reflections were not split because a certain fraction of chains bridging these lamellae constrained the interlamellar gap spacing.²⁰ After all bridging chains reptated to respective lamellae (Figure 5c), the pattern in Figure 3c was observed. The strong reflections were split when the interlamellar gap was not simply related to the chain methylene repeat.

The one-dimensional Fourier transforms of 00/ rows calculated for averaged similar diffraction patterns from local microcrystalline domains, representing C40 to C44 lamellae, each indicated that a continuous carbon chain should run through the crystal structure. In the one-dimensional potential maps, the principal indicator of a nascent lamellar structure was the clustered fractional occupancies of some carbon positions.

A data set was formed by averaging intensities in $0k/$ patterns from a number of C41-like layers. An atomic model was constructed in space group Aa , placing the middle carbon at $z/c = 0.25$. (This is equivalent to constructing a $A2_1am$ layer packing since the chain carbon is on a defined mirror position.¹⁸) The chain atom

Table 1. Carbon Chain Model for the PE600 Most Resembling n -C₄₁H₈₄

| x/a | y/b | z/c | occ | x/a | y/b | z/c | occ |
|-------|-------|-------|------|-------|-------|-------|------|
| 0.119 | 0.309 | 0.017 | 0.89 | 0.037 | 0.190 | 0.262 | 1.00 |
| 0.037 | 0.190 | 0.029 | 0.90 | 0.119 | 0.309 | 0.273 | 1.00 |
| 0.119 | 0.309 | 0.041 | 0.91 | 0.037 | 0.190 | 0.285 | 1.00 |
| 0.037 | 0.190 | 0.052 | 0.92 | 0.119 | 0.309 | 0.297 | 1.00 |
| 0.119 | 0.309 | 0.064 | 0.95 | 0.037 | 0.190 | 0.308 | 1.00 |
| 0.037 | 0.190 | 0.076 | 0.98 | 0.119 | 0.309 | 0.320 | 1.00 |
| 0.119 | 0.309 | 0.087 | 1.00 | 0.037 | 0.190 | 0.331 | 1.00 |
| 0.037 | 0.190 | 0.099 | 1.00 | 0.119 | 0.309 | 0.343 | 1.00 |
| 0.119 | 0.309 | 0.110 | 1.00 | 0.037 | 0.190 | 0.355 | 1.00 |
| 0.037 | 0.190 | 0.122 | 1.00 | 0.119 | 0.309 | 0.366 | 1.00 |
| 0.119 | 0.309 | 0.134 | 1.00 | 0.037 | 0.190 | 0.378 | 1.00 |
| 0.037 | 0.190 | 0.145 | 1.00 | 0.119 | 0.309 | 0.390 | 1.00 |
| 0.119 | 0.309 | 0.157 | 1.00 | 0.037 | 0.190 | 0.401 | 1.00 |
| 0.037 | 0.190 | 0.169 | 1.00 | 0.119 | 0.309 | 0.413 | 1.00 |
| 0.119 | 0.309 | 0.180 | 1.00 | 0.037 | 0.190 | 0.424 | 0.98 |
| 0.037 | 0.190 | 0.192 | 1.00 | 0.119 | 0.309 | 0.436 | 0.95 |
| 0.119 | 0.309 | 0.203 | 1.00 | 0.037 | 0.190 | 0.448 | 0.92 |
| 0.037 | 0.190 | 0.215 | 1.00 | 0.119 | 0.309 | 0.459 | 0.91 |
| 0.119 | 0.309 | 0.227 | 1.00 | 0.037 | 0.190 | 0.471 | 0.90 |
| 0.037 | 0.190 | 0.238 | 1.00 | 0.119 | 0.309 | 0.483 | 0.89 |
| 0.119 | 0.309 | 0.250 | 1.00 | | | | |

model was then extended along c by increments of $c_s/2 = 1.275$ Å to construct a 41-carbon layer. (Here, $c_s = 2.55$ Å is the chain zigzag repeat of high molecular weight polyethylene or the chain axis of the O_\perp methylene subcell.²¹) However, the gaps between layers was defined to be $3(c_s/2) = 3.82$ Å, i.e., an integral number of methylene repeats. For this example, the resultant layer repeat would be 54.82 Å vs a measured value of 54.90(37) Å. The orthorhombic unit cell constants would therefore be $a = 7.42$, $b = 4.96$, and $c = 109.65$ Å. Fractional carbon positions of the molecular model are listed in Table 1 along with partial occupancies near the chain ends at positions indicated by the one-dimensional transform. Idealized hydrogen atom positions were added.

For 20 observed $0kl$ reflections from this local lamellar packing, a structure factor calculation based on the layer model ($B_C = 4.0$, $B_H = 6.0$ Å²) gives a very good fit ($R = 0.21$). These values are compared in Table 2. Although the model in Table 1 is a discontinuous layer structure, the potential maps made from the phased structure factors (Figure 6) indicate a small population of continuous carbon chains extending across the lamellar interface. (It should be emphasized that the chain model was an idealized rigid body so that an fractional atomic occupancy envelope and overall temperature factors for the two atom types were the only variables in this determination. The model, therefore, was not over-parametrized.)

Discussion

From the analyses of diffraction data from oriented low molecular weight linear polyethylene, it is clear that its crystal structure is quite distinct from that found for the refined petroleum wax fractions,^{5,11,12} which are characterized by a Gaussian distribution of chain lengths in the polydisperse solid solution.²² This polyethylene structure is more akin to the chain packing observed when very long chain-extended paraffins, crystallized from the vapor phase, are annealed toward a final stable lamellar structure.²⁰ Its intrinsically lamellar nature had been indicated before by electron micrographs from chain-extended samples, as well as by Raman LAM measurements.²³ However, this structure analysis reveals that there must be a population of very long chain

Table 2. Final Observed and Calculated Structure Factors for PE600

| hkl | $ F_{\text{obs}} $ | $ F_{\text{calc}} $ | hkl | $ F_{\text{obs}} $ | $ F_{\text{calc}} $ |
|-------|--------------------|---------------------|-------|--------------------|---------------------|
| 00 2 | 0.52 | 0.51 | 02 2 | 0.23 | 0.13 |
| 00 4 | 0.40 | 0.45 | 02 4 | 0.15 | 0.11 |
| 00 6 | 0.24 | 0.36 | 02 84 | 0.09 | 0.03 |
| 00 84 | 0.11 | 0.08 | 02 86 | 0.54 | 0.36 |
| 00 86 | 0.80 | 0.92 | 02 88 | 0.09 | 0.02 |
| 00 88 | 0.11 | 0.05 | 03 41 | 0.11 | 0.06 |
| 01 41 | 0.18 | 0.11 | 03 43 | 0.77 | 0.73 |
| 01 43 | 1.03 | 1.34 | 03 45 | 0.08 | 0.04 |
| 01 45 | 0.14 | 0.08 | 04 0 | 0.25 | 0.22 |
| 02 0 | 2.01 | 1.87 | 05 43 | 0.47 | 0.20 |

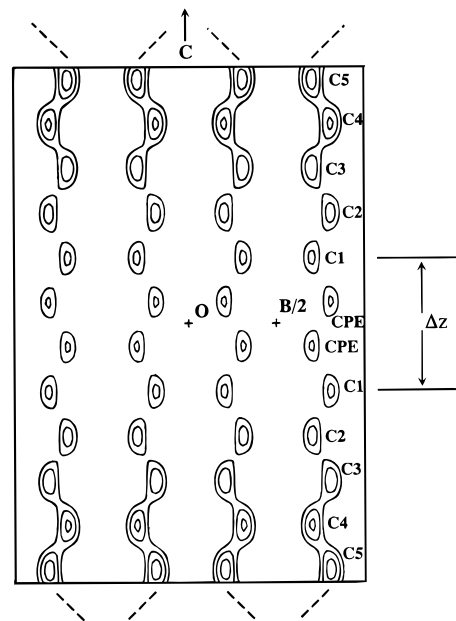


Figure 6. Potential map for the C41-like layers in PE600, emphasizing the lamellar interface. The gap Δz between lamellae is indicated. Although only 41 carbons were used in the crystal structure model (Table 1), the map obtained with calculated crystallographic phases and experimental amplitudes indicates two additional methylene units (CPE) bridging the gap. This is taken to signify the presence of longer chain components spanning nascent lamellae. The positions of the first five carbons (C_m) in unique chains of each lamella are also indicated (see Table 1 for coordinates). The number of contours for each carbon would be roughly proportional to its atomic occupancy factor.

components that prevent the total separation of a lamellar structure.²⁰ The bridging molecules impose a gap of 3.82 Å between the nascent lamellae, which is an integral multiple of the chain carbon repeat along the c -axis. The usual dimension for this gap in n -paraffins is about 3.16 Å, differing enough from the other value to cause the most intense polyethylene reflections to split into two intense peaks, due to the scattering interference between two off-set carbon chain gratings.

The postulated longer chain components can, in fact, be found for the natural waxes, e.g., those from bee honeycomb.¹¹ Do they, in fact, also exist for the chain-extended polyethylenes? In an earlier paper, Prasad and Mandelkern²⁴ analyzed the same polyethylene product used for this study. In a separate analysis of the number-average molecular weight by ¹H or ¹³C NMR, they determined values of 560 and 530, respectively. However, they were also able to isolate a separate fraction from this polyethylene with a number-average molecular weight of 800. This would correspond to a

chain length of about 57 carbons. Since the largest average lamellar thickness observed in this work was about 44 carbons, there must be enough longer (unfolded, linear) chains that bridge the emergent lamellae to prevent them from fully separating. A broad range of chain distributions in a skewed Gaussian distribution is also found in Raman LAM measurements on other extended chain linear low molecular weight polyethylenes with similarly low polydispersity.²³

A compact lamellar structure with longer chains protruding into adjacent lamellae is consistent with earlier interpretations²⁵ of ¹³C NMR measurements from PE740. However, the presence of these bridging molecular chain ties between lamellae raises other questions. For example, when this chain length fraction is crystallized from solution and then decorated with polyethylene vapors, there seems to be enough crystalline perfection in the (001) surface to epitaxially nucleate the deposited chains.⁹ Are the longer chain cilia then sequestered laterally to separate domains? Such crystallites are often conceived to be "fringed" lamellae containing a compact crystalline core and two amorphous surface layers.²⁶ Electron microscopy of some chain-extended polyethylene samples reveals the separation of some individual lamellae grown from solution,²³ but there are also more ordered lamellar stacks. Is the disorder in the longer chain ends, therefore, dependent on the mode of crystallization (solution or melt)? These questions, as well as a more quantitative assessment of chain composition in these polyethylenes, will be addressed in future studies.

Acknowledgment. Research was supported by a grant from the National Science Foundation (CHE-9730317) which is gratefully acknowledged. The author is grateful for helpful discussions with Prof. Leo Mandelkern.

References and Notes

- (1) Dorset, D. L. *Proc. Natl. Acad. Sci. U.S.A.* **1990**, *87*, 8541.
- (2) Dorset, D. L. *Z. Kristallogr.*, in press.
- (3) Dorset, D. L.; Hanlon, J.; Karet, G. *Macromolecules* **1989**, *22*, 2169.
- (4) Wittmann, J. C.; Hodge, A. M.; Lotz, B. *J. Polym. Sci., Polym. Phys. Ed.* **1983**, *21*, 2495.
- (5) Dorset, D. L. *Macromolecules* **1987**, *20*, 2782.
- (6) Kitaigorodskii, A. I. *Organic Chemical Crystallography*; Consultants Bureau: New York, 1961; p 231ff.
- (7) Lüth, H.; Nyburg, S. C.; Robinson, P. M.; Scott, H. G. *Mol. Cryst. Liq. Cryst.* **1974**, *27*, 337.
- (8) Gerson, A. R.; Nyburg, S. C. *Acta Crystallogr.* **1994**, *B50*, 252.
- (9) Dorset, D. L.; Annis, B. K. *Macromolecules* **1996**, *29*, 2969.
- (10) Maroncelli, M.; Strauss, H. L.; Snyder, R. G. *J. Phys. Chem.* **1985**, *89*, 5260.
- (11) Dorset, D. L. *Acta Crystallogr.* **1995**, *B51*, 1021.
- (12) Dorset, D. L. *J. Phys. D: Appl. Phys.* **1997**, *30*, 451.
- (13) Dorset, D. L. *Z. Kristallogr.*, in press.
- (14) Dorset, D. L. *Structural Electron Crystallography*; Plenum: New York, 1995.
- (15) Nyburg, S. C.; Potworowski, J. A. *Acta Crystallogr.* **1973**, *B29*, 347.
- (16) Retief, J. J.; Engel, D. W.; Boonstra, E. G. *J. Appl. Crystallogr.* **1985**, *18*, 156.
- (17) Dorset, D. L.; McCourt, M. P.; Li, G.; Voigt-Martin, I. G. *J. Appl. Crystallogr.* **1998**, *31*, 544.
- (18) Hahn, T., Ed. *International Tables for Crystallography*; Kluwer: Dordrecht, 1995; Vol. A.
- (19) Dorset, D. L.; Zemlin, F. *Ultramicroscopy* **1990**, *33*, 227.
- (20) Dorset, D. L.; Zhang, W. P. *J. Electron Microsc. Technol.* **1991**, *18*, 142.
- (21) Zhang, W. P.; Dorset, D. L. *J. Polym. Sci. B, Polym. Phys.* **1990**, *28*, 1223.
- (22) Hu, H. L.; Dorset, D. L. *Acta Crystallogr.* **1989**, *B45*, 283.
- (23) Basson, I.; Reynhardt, E. C. *Chem. Phys. Lett.* **1992**, *198*, 367.
- (24) Stack, G. M.; Mandelkern, L.; Voigt-Martin, I. G. *Macromolecules* **1984**, *17*, 321.
- (25) Prasad, A.; Mandelkern, L. *Macromolecules* **1989**, *22*, 914.
- (26) Russell, K. F.; Wu, G.; Blake, S.; Heyding, R. D. *Polymer* **1992**, *33*, 951.
- (27) Möller, M.; Cantow, H. J.; Drotloff, H.; Emeis, D.; Lee, K. S.; Wegner, G. *Makromol. Chem.* **1986**, *187*, 1237.

MA981371R